INTERNATIONAL JOURNAL OF OPTIMIZATION IN CIVIL ENGINEERING
Int. J. Optim. Civil Eng., 2015; 5(3):267-282

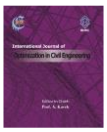

PREDICTION OF EARTHQUAKE INDUCED DISPLACEMENTS OF SLOPES USING HYBRID SUPPORT VECTOR REGRESSION WITH PARTICLE SWARM OPTIMIZATION

H. Fattahi[*, †]
Department of Mining Engineering, Arak University of Technology, Arak, Iran

ABSTRACT

Displacements induced by earthquake can be very large and result in severe damage to earth and earth supported structures including embankment dams, road embankments, excavations and retaining walls. It is important, therefore, to be able to predict such displacements. In this paper, a new approach to prediction of earthquake induced displacements of slopes (EIDS) using hybrid support vector regression (SVR) with particle swarm optimization (PSO) is presented. The PSO is combined with the SVR for determining the optimal value of its user-defined parameters. The optimization implementation by the PSO significantly improves the generalization ability of the SVR. In this research, the input data for the EIDS prediction consist of values of geometrical and geotechnical input parameters. As an output, the model estimates the EIDS that can be modeled as a function approximation problem. A dataset that includes 45 data points was applied in current study, while 36 data points (80%) were used for constructing the model and the remainder data points (9 data points) were used for assessment of degree of accuracy and robustness. The results obtained show that the SVR-PSO model can be used successfully for prediction of the EIDS.

Received: 10 March 2015; Accepted: 20 May 2015

KEY WORDS: earthquake; support vector regression (SVR); particle swarm optimization (PSO); displacement; slope.

1. INTRODUCTION

Field observations show that landslides of man-made and natural slopes in strong earthquakes are common phenomena [1]. Earthquakes with magnitudes greater than 4.0 can

[*]Corresponding author: Department of Mining Engineering, Arak University of Technology, Arak, Iran
[†]E-mail address: H.fattahi@arakut.ac.ir (H. Fattahi)

cause landslides on very susceptible slopes, and earthquakes with magnitudes greater than 6.0 can generate widespread landsliding [2, 3]. Whether a particular slope produces a landslide in an earthquake depends on details of slope configuration, material strength and ground motion [1].

Deformations triggered by earthquakes in man-made and natural slopes may develop in three consequent stages.

In the first stage, which is co-seismic, gravity as well as seismic forces, which during the relatively short duration of an earthquake may bring about instability, can generate a failure surface or active a pre-existing slip plane causing permanent displacements of the slope. Co-seismic displacements, unless the residual strength of the material in which they occur drops to very low values, are usually small and are controlled by the magnitude and duration of the application of the earthquake inertia forces, the geometry of the slope, and the undrained strength of the material mobilized during the earthquake.

The second stage, which is post-seismic, follows immediately after the earthquake if the fast residual undrained shear strength on the slip surface generated by the shock is less than that required to maintain static equilibrium; i.e. if the initial safety factor (SF) of the slope, SF at the end of the earthquake is less than one. A drop in resisting forces will thus lead to an acceleration of the mass downslope. In this case, down-slope displacements, initiated by the earthquake will continue with an outward movement of the toe, the velocity of motion providing the kinetic energy necessary for further transport of slide material. As a result of this, when the mass comes to rest in a new position of equilibrium, its SF will be greater than one.

A third stage of displacements, which is not examined here, may follow. In this stage further movements may develop as a result of creep and consolidation processes, as well as from destabilizing hydrostatic forces if deep open cracks produced by the shock are filled with surface or ground water [1]. Additional movements may occur, which will be slow and associated with progressive failure and drained strength of the soil. This third stage may follow immediately the first stage if, at the end of the earthquake, the post-seismic static SF is close to one, or if the residual factor is less than one. Several methods for the evaluation of first first-stage, co-seismic displacements have been proposed [4-8]. The extension of the evaluation of co-seismic displacements into the second stage has also been studied [9-11].

In the field of EIDS modeling, although previous efforts are valuable and revealed the better performance of intelligence-based models in preference to scaling equation, the pursuit of the novel model introduction with more accurate results is always ongoing. The SVR is a potent data mining model, which was developed by Vapnik [12] and co-workers based on statistical learning theory for solving problems encountered in petroleum industry. Although this method is a powerful methodology for modeling of different phenomena, it suffers from some shortcomings, which limit its application. In every the SVR modeling, a series of user-defined parameters exist that required to be chosen by user precisely. Incorrect input of aforementioned parameters by user can lead to erroneous and even deceptive results. Hence, it is crucial to employ a potent optimization algorithm for searching the proper value of these parameters [13, 14]. By now, there have been several optimization algorithms, such as genetic algorithm (GA) inspired by the Darwinian law of survival of the fittest [15], ant colony optimization (ACO) inspired by the foraging behavior of ant colonies [16], biogeography-based optimization (BBO) inspired by the migration behavior of island

species. Also, recently new optimization algorithms are developed consisting of charged system search (CSS) [17], ray optimization (RO) [18], democratic particle swarm optimization (DPSO) [19], colliding bodies optimization (CBO) [20] and enhanced colliding bodies optimization (ECBO). In present paper, for the achievement of the above mentioned purpose, a fast, robust, and easy to used method so-called particle swarm optimization (PSO) is applied as the searching strategy for finding the optimal value of user-defined parameters. Indeed, PSO is capable of improving the performance of SVR through determining their free parameters. Integration of SVR model and PSO method produced a model, which can predict the EIDS with good precision.

2. A BRIEF REVIEW OF METHODS USED IN THIS STUDY

2.1 Support vector regression

Support vector machines (SVMs), was introduced as a machine learning technique by Vapnik [12], have received so much attention due to their promising capabilities in simultaneous and prediction error minimization since its development [21-23]. The underlying concept of support vector regression (SVR) is to map the original data into a higher-dimensional feature space and to fit a linear function with least reasonable complexity to the feature space [24, 25]. The latter stage is as well as making the function as flat as possible to reduce the complexity and means better generalization to a considerable extent.

Let the training samples be denoted as $XY = \{(x, y) \mid (x_1, y_1), ..., (x_n, y_n)\}$ where n is the number of training samples. In SVR, the ultimate goal is to find linear relation between n-dimensional input vectors $x \in R^n$ and output variables $y \in R$ as follow:

$$f(x) = w^T x + b \tag{1}$$

Where, b and w are offset of the regression line and the slope respectively. For determining the values of b and w, it is necessary to minimize following equation:

$$R = \frac{1}{2}\|w\|^2 + \frac{C}{l}\sum_{i=1}^{l} |y_i - f(x_i)|_{\varepsilon} \tag{2}$$

Loss function, utilized in SVR is ε-insensitive which has been proposed by Vapnik (1995) [12] as below:

$$|y_i - f(x_i)|_{\varepsilon} = \begin{cases} 0 & if \quad |y_i - f(x_i)| \le \varepsilon \\ |y_i - f(x_i)| - \varepsilon & Otherwise \end{cases} \tag{3}$$

This problem can be reformulated in a dual space by:

$$Maximize\, L_p(\alpha_i, \alpha_i^*) = -\frac{1}{2}\sum_{i,j=1}^{l}(\alpha_i - \alpha_i^*)(\alpha_j - \alpha_j^*)\, x_i^T x_j - \varepsilon\sum_{i=1}^{l}(\alpha_i + \alpha_i^*) + \sum_{i=1}^{l}(\alpha_i - \alpha_i^*)\, y_i \tag{4}$$

$$Subject\ to \begin{cases} \sum_{i=1}^{l}(\alpha_i - \alpha_i^*) = 0 \\ 0 \le \alpha_i \le C, \quad i = 1,...,l \\ 0 \le \alpha_i^* \le C, \quad i = 1,...,l \end{cases} \tag{5}$$

Where, $\alpha_i, \alpha_i^* \ge 0$ are positive Lagrange multipliers. C is regulated positive parameter which determines trade-off between approximation error and the weight vector norm $\|w\|$. After calculation of Lagrange multipliers α_i and α_i^*, training data points, those meeting the conditions $\alpha_i - \alpha_i^* \ne 0$, will be applied to construct the decision function. Hence, the best linear hyper surface regression is given by:

$$f(x) = w_0^T x + b = \sum_{i=1}^{l}\left(\alpha_i - \alpha_i^*\right)x_i^T x + b \tag{6}$$

Which desired weight vector of the regression hyper plane is given by:

$$w_0 = \sum_{i=1}^{l}\left(\alpha_i - \alpha_i^*\right)x_i \tag{7}$$

In nonlinear regression, Kernel function is applied for mapping input data onto higher dimensional feature space in order to generate a linear regression hyper plane. In the case of the nonlinear regression, the learning problem is again formulated in the same way as in a linear case, i.e., the nonlinear hyperplane regression function becomes:

$$f(x) = \sum_{i=1}^{l}\left(\alpha_i - \alpha_i^*\right)K(x_i, x) + b \tag{8}$$

Where, $K(x_i, x)$ is kernel function which is defined as follow:

$$K(x_i, x_j) = \Phi^T(x_i)\Phi(x_j) \qquad i, j = 1,...,l \tag{9}$$

Where, $\Phi(x_i)$ and $\Phi(x_j)$ are projection of the x_i and x_j in feature space respectively.

One may choose any arbitrary kernel functions, e.g., linear kernel function $K\left(x_i, x_j\right) = \left(x_i, x_j\right)$, radial basis function (RBF) $K\left(x_i, x_j\right) = \exp(-\left\|x_i - x_j\right\|/2\sigma^2), \sigma > 0$, polynomial kernel function $K\left(x_i, x_j\right) = (\left(x_i, x_j\right)+1)^d, d > 0$, etc. In highly non-linear spaces, RBF kernel usually yields more promising results in comparison with other mentioned

kernels [26]. Thus, we use only RBF kernel functions in this study.

2.2 Particle swarm optimization

The PSO is one of the recent evolutionary optimization methods. This technique was firstly suggested by Eberhart and Kennedy [27] in order to solve problems with continuous search space. The PSO is based on the metaphor of communication and social interaction, such as bird flocking and fish schooling. The PSO uses social rules to search in the design space by controlling the trajectories of a set of independent particles. The position of each particle, x_i, representing a particular solution of the problem, is used to compute the value of the fitness function to be optimized. Each particle may change its position and consequently may explore the solution space, simply varying its associated velocity. In fact, the main the PSO operator is the velocity update, which considers the best position, in terms of fitness value reached by all the particles during their paths, P_g^t, and the best position that the agent itself has reached during its search, P_i^t, resulting in a migration of the entire swarm toward the global optimum.

At each iteration the particle moves around according to its velocity and position; the cost function to be optimized is evaluated for each particle in order to rank the current location. The position of each particle is updated using its velocity vector as shown in Eq. (2) and depicted in Fig. 1.

$$V_i^{t+1} = \omega V_i^t + C_1 r_1^t (P_i^t - X_i^t) + C_2 r_2^t (P_g^t - X_i^t) \tag{10}$$

$$X_i^{t+1} = X_i^t + V_i^{t+1} \tag{11}$$

where, V_i^t is the velocity vector at iteration t, $r_1$and r_2 represents random numbers in the range [0,1]; P_g^t denotes the best ever particle position of particle i, and P_i^t corresponds to the global best position in the swarm up to iteration t [28]. The remaining terms are problem-dependent parameters; for example, C_1 and C_2 represent "trust" parameters indicating how much confidence the current particle has in itself (C_1: cognitive parameter) and how much confidence it has in the swarm (C_2: social parameter), and ω is the inertia weight.

The PSO algorithm has several advantages including: PSO is based on the intelligence. It can be applied into both scientific research and engineering use. Then PSO have no overlapping and mutation calculation. The search can be carried out by the speed of the particle. During the development of several generations, only the most optimist particle can transmit information onto the other particles, and the speed of the researching is very fast. After that the calculation in PSO is very simple. Compared with the other developing calculations, it occupies the bigger optimization ability and it can be completed easily. The last one is PSO adopts the real number code, and it is decided directly by the solution. The number of the dimension is equal to the constant of the solution [29].

Recently, the PSO was used in different applications by various researchers worldwide [30-33].

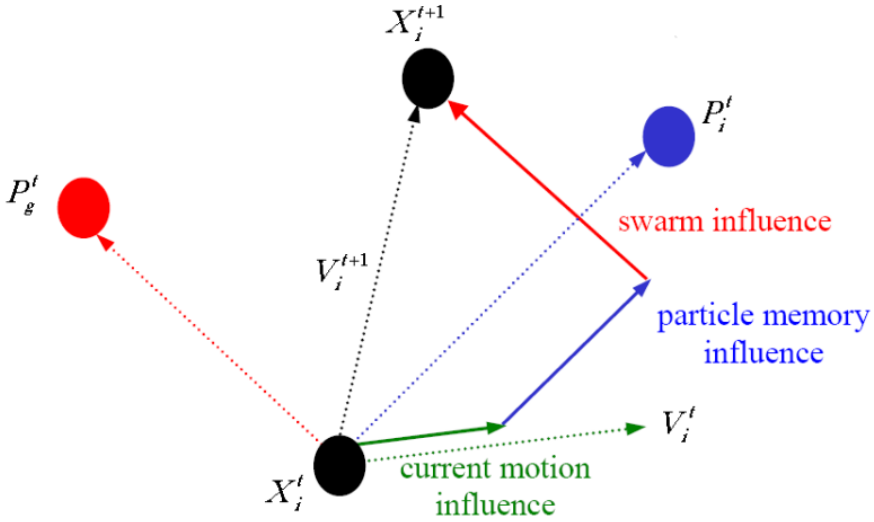

Figure 1. Depiction of the velocity and position updates in PSO

3. PARAMETERS OPTIMIZATION OF THE SVR BASED ON PSO

The generalization ability of the SVR is extremely dependent upon its learning parameters, i.e., the RBF kernel parameter $\sigma \in \left[2^{-5}, 2^{5}\right]$, the error margin $\varepsilon \in [0.01, 0.6]$, and the regularization parameter $C \in \left[2^{-5}, 2^{15}\right]$, to be set correctly. Finding the best combination of hyper-parameters is often troublesome due to the highly non-linear space of the model performance with respect to these parameters. Although an exhaustive search method could be utilized to tune these hyper-parameters, it suffers from the main drawbacks of being very time-consuming and lacking a guarantee of convergence to the globally optimal solution. For example, the real-value genetic algorithm (GA) was employed to determine the optimal parameters of SVR, which were then applied to construct the SVR model, referred to as SVR-GA [34-36]. The ACO has also been used to select the model parameters of SVR by several researchers [37-39]. Recently, the harmony search (HS) has also been utilized to select the model parameters of SVR [40].

In this paper, we have adopted the PSO for optimal parameter selection of SVR in order to improve runtime efficiency of learning procedure of SVR– PSO. Fig. 2 shows the algorithm process of the selection of the SVR model parameters based on PSO.

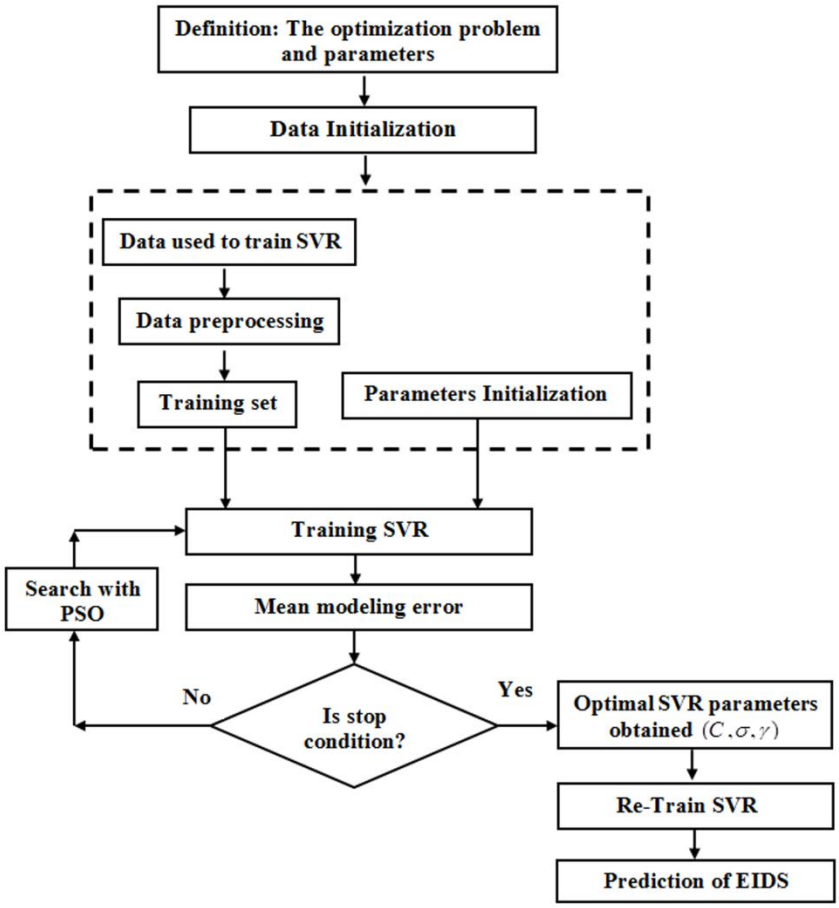

Figure 2. The process of optimizing the SVR parameters with the PSO

4. INPUT/ OUTPUT DATA SPACE

The main scope of this study is to implement the above methodology in the problem of the earthquake induced displacements prediction for slopes. Dataset applied in this study for determining the relationship among the set of input and output variables are gathered from open source literature [41]. The original data covering the 45 case studies are presented in Table 1 that 36 cases (80%) were used for training and 9 cases (20%) were used for testing. The data sets in Table 1 was created through processing of an initial data set referring to five typical embankments of slope angle β= 2:3 and pore water pressure ratio r_u=0.1. These embankments were studied in order to determine the static safety factor F, the critical acceleration coefficient (k_y), and the earthquake induced displacement u due to an earthquake of certain magnitude. A computer program was written in MATLAB environment in order to calculate induced displacements for r = 5, 10, 15 km and M=6, 6.5 and 7 Richter. The datasets in Table 1 contains data for 45 slopes, were u was calculated through the use of Eqs. (12) to (14). The formulation of the problem in the current example case refers to the mapping of the parameters: height (H), unit specific weight (γ), cohesion

(c), angle of internal friction (φ), significant duration of shaking ($D_{5–95}$), maximum horizontal acceleration (k_{max}) to displacement (u).

$$\log_{10}\left(\frac{u}{k_{\max}D_{5–95}}\right)=1.87-3.477\frac{k_y}{k_{\max}} \tag{12}$$

Where $D_{5–95}$: significant duration of shaking, i.e., 5–95% normalized Arias intensity (sec), $K_{\max}=\frac{MHEA}{g}$ ($MHEA$: maximum horizontal equivalent acceleration, characterizes the amplitude of shaking within the sliding mass) and k_y: yield acceleration of the slope [41].

$$\ln\left(D_{5–95}\right)_{med}=\ln\left[\frac{\left(\frac{\exp\left[5.204+0851(M-6)\right]}{10^{1.5M+16.05}}\right)^{-\frac{1}{3}}}{15.7\times10^{6}}+0.0063\left(r-10\right)\right]+0.8664, \qquad For\ r\succ10km \tag{13}$$

$$\ln\left(D_{5–95}\right)_{med}=\ln\left[\frac{\left(\frac{\exp\left[5.204+0851(M-6)\right]}{10^{1.5M+16.05}}\right)^{-\frac{1}{3}}}{15.7\times10^{6}}\right]+0.8664, \qquad For\ r\prec10km \tag{14}$$

Where M: earthquake magnitude and r: distance in km [41].

Table 1: The original data were used for training and testing model [41]

Case No.	Input parameters						Output parameter
	H (m)	ɣ (KN/m^3)	C (KPa)	Φ (^{o})	$D_{5–95}$	k_{max}	u (cm)
1	12	22	8	35	7.9	0.24	0.25
2	12	22	8	35	8.35	0.2	0.06
3	12	22	8	35	9.55	0.13	0.0008
4	12	22	8	35	11.1	0.33	2.7
5	12	22	8	35	11.5	0.27	0.82
6	12	22	8	35	12.7	0.18	0.036
7	12	22	8	35	16	0.45	18.16
8	12	22	8	35	16.4	0.37	7.37
9	12	22	8	35	17.65	0.24	0.55
10	10	22	5	35	7.9	0.24	1.19
11	10	22	5	35	8.35	0.2	0.4
12	10	22	5	35	9.55	0.13	0.014
13	10	22	5	35	11.1	0.33	8.45

14	10	22	5	35	11.5	0.27	3.31
15	10	22	5	35	12.7	0.18	0.3
16	10	22	5	35	16	0.45	42
17	10	22	5	35	16.4	0.37	20.4
18	10	22	5	35	17.65	0.24	2.7
19	10	21	5	36	7.9	0.24	0.55
20	10	21	5	36	8.35	0.2	0.16
21	10	21	5	36	9.55	0.13	0.003
22	10	21	5	36	11.1	0.33	4.84
23	10	21	5	36	11.5	0.27	1.68
24	10	21	5	36	12.7	0.18	0.1
25	10	21	5	36	16	0.45	27.84
26	10	21	5	36	16.4	0.37	12.4
27	10	21	5	36	17.65	0.24	1.24
28	8	22	6	36	7.9	0.24	0.094
29	8	22	6	36	8.35	0.2	0.02
30	8	22	6	36	9.55	0.13	0.0001
31	8	22	6	36	11.1	0.33	1.34
32	8	22	6	36	11.5	0.27	0.35
33	8	22	6	36	12.7	0.18	0.001
34	8	22	6	36	16	0.45	10.8
35	8	22	6	36	16.4	0.37	3.94
36	8	22	6	36	17.65	0.24	0.2
37	6	21	5	35	7.9	0.24	0.07
38	6	21	5	35	8.35	0.2	0.013
39	6	21	5	35	9.55	0.13	7.34
40	6	21	5	35	11.1	0.33	1.07
41	6	21	5	35	11.5	0.27	0.26
42	6	21	5	35	12.7	0.18	0.006
43	6	21	5	35	16	0.45	9.24
44	6	21	5	35	16.4	0.37	3.24
45	6	21	5	35	17.65	0.24	0.16

4. PREDICTION OF EARTHQUAKE INDUCED DISPLACEMENTS OF SLOPES

4.1 Pre-processing of data

In data-driven system modeling methods, some pre-processing steps are usually implemented prior to any calculations, to eliminate any outliers, missing values or bad data. This step ensures that the raw data retrieved from database is perfectly suitable for modeling. In order to soften the training procedure and improve the accuracy of estimation, all data samples are normalized to adapt to the interval [-1, 1] according to the following linear mapping function:

$$x_M = 2\left(\frac{x - x_{\min}}{x_{\max} - x_{\min}}\right) - 1 \tag{15}$$

Where x is the original value of the dataset, x_M is the mapped value, and x_{max} (x_{min}) denotes the maximum (minimum) raw input values, respectively.

4.2 Evaluation criteria

To verify the performance of the model, four statistical criteria viz. mean squared error (MSE), variance account for (VAF), root mean squared error (RMSE), squared correlation coefficient (R^2) and mean absolute percentage error (MAPE) were chosen to be the measure of accuracy. Let t_k be the actual value and $\hat{t}_k$ be the predicted value of the k^{th} observation and n be the number of observations, then RMSE, MSE, VAF, R^2 and MAPE could be defined, respectively, as follows:

$$MSE = \frac{1}{n}\sum_{k=1}^{n}(t_k - \hat{t}_k)^2 \tag{16}$$

$$VAF = \left(1 - \frac{\text{var}(t_k - \hat{t}_k)}{\text{var}(t_k)}\right) \tag{17}$$

$$RMSE = \sqrt{\frac{1}{n}\sum_{k=1}^{n}(t_k - \hat{t}_k)^2} \tag{18}$$

$$R^2 = \frac{(\sum_{k=1}^{n} t_k \hat{t}_k - n\mu_t \mu_{\hat{t}})^2}{(\sum_{k=1}^{n} \hat{t}_k^{\,2} - n\mu_t^{\,2})^2 (\sum_{k=1}^{n} \hat{t}_k^{\,2} - n\mu_{\hat{t}}^{2})^2} \tag{19}$$

$$MAPE = \frac{1}{n}\sum_{k=1}^{n}\left|\frac{t_k - \hat{t}_k}{t_k}\right| \times 100 \tag{20}$$

Where μ_t ($\mu_{\hat{t}}$) denotes the mean value of the μ_k ($\mu_{\hat{k}}$), $k = 1, ..., n,$ respectively.

4.3 Results and discussion

In this paper, a hybrid SVR with PSO was proposed to predict the EIDS, using MATLAB environment. Fig. 3 shows the architecture of the SVR-PSO model used. As it can be seen in Fig. 3, height (H), unit specific weight (γ), cohesion (c), angle of internal friction (φ), significant duration of shaking (D_{5-95}), maximum horizontal acceleration (k_{max}) were defined as input parameters into the SVR-PSO model and the displacement as output.

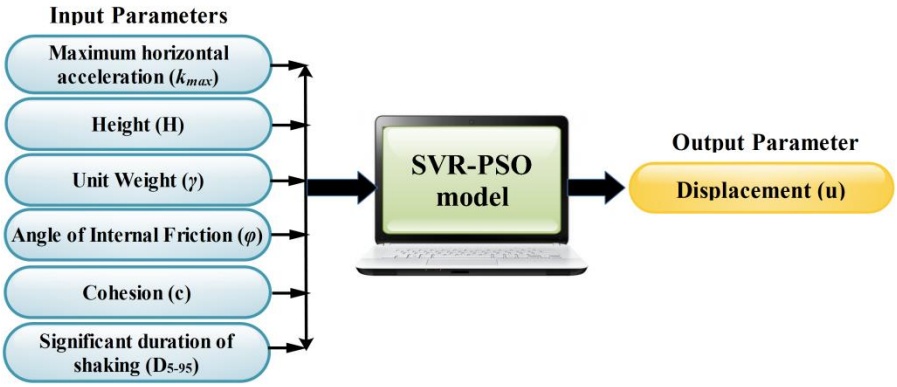

Figure 3. Architecture of the SVR-PSO model

Furthermore, as shown in section 2.1, the generalization ability of SVR is highly dependent upon its learning parameters, i.e., $\{C, \sigma, \varepsilon\}$. Consequently, the PSO was used to manipulate these parameters and to form hybrid SVR– PSO. 10-fold cross-validation performance measure was applied to training dataset along with SVR– PSO to achieve reliable results. Related to the purpose, the PSO algorithm with number of population (swarm size) =100, personal learning coefficient=1.4962, global learning coefficient=1.4962, inertia weights =0.73 and the algorithm was executed for 100 iterations for selecting optimal parameters. The adjusted parameters $\{C, \sigma, \varepsilon\}$ with maximal accuracy are selected as the most appropriate parameters. Then, the optimal parameters are used to train the SVR model. The accuracy and optimal parameters of the SVR estimated by the PSO are presented in Table 2.

Table 2: The accuracy and optimal parameters of the SVR estimated by the PSO

	Optimal value of σ parameter	Optimal value of C parameter	Optimal value of ε parameter
SVR-PSO model	1.8164	1844.808	0.029

The obtained RMSE, MSE, VAF, R^2 and MAPE values for training datasets indicate the ability of learning the structure of data samples, while the results of testing dataset reveal the generalization potential and the robustness of the system modeling methods. The learning capacity of a model is considerably contingent upon the built-in system complexity, which implies the number of free parameters available for learning from the particularities of the

training dataset. This learning potential, alone, could not assure a promising generalization capability for a model. It is clear that as the complexity of system increases, the model errors for training samples (empirical risks) decrease despite the fact that the over-fitting risk multiplies rapidly. Thus, based on structure risk minimization theorem, empirical risks and complexity risks must be minimized simultaneously for designing reliable, efficient, and robust models.

A comparison between predicted values of displacement by the SVR-PSO model and measured values for 45 data sets at training and testing phases is shown in Figs. 4 and 5. As shown in Figs. 4 and 5, the results of the SVR-PSO modeling compared with actual data show a good precision of the SVR-PSO model (see Table 3).

Performance analysis of the SVR-PSO model for predicting displacement is shown in Table 3.

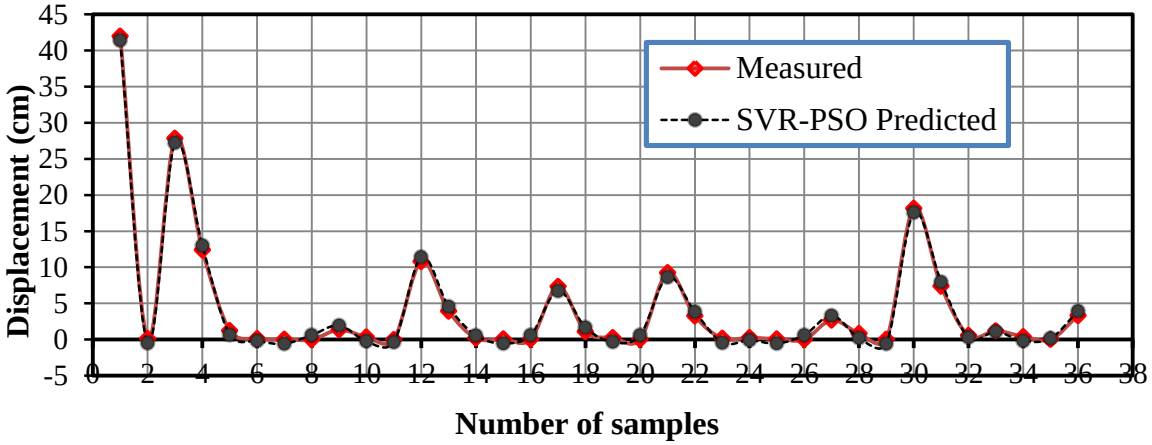

Figure 4. Comparison between measured and predicted displacement for training data points

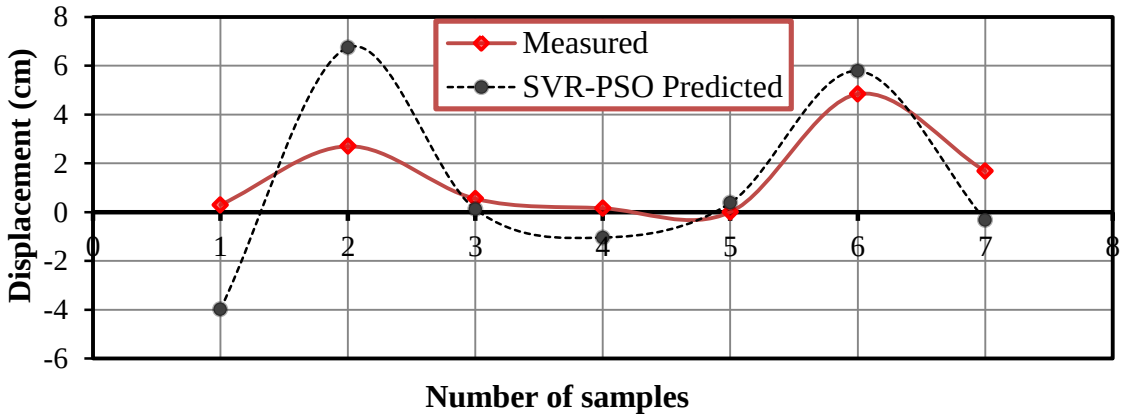

Figure 5. Comparison between measured and predicted displacement for testing data points

Table 3: Performance of the model for predicting displacement

Description	R^2	MSE	RMSE	VAF	MAPE
Training	0.9959	0.00068	0.026	99.58	3.4537
Testing	0.9333	0.0146	0.1209	83.53	82.663

The performance indices obtained in Table 3 indicate the high performance of the SVR-PSO model that can be used successfully to prediction of the EIDS. Furthermore, the correlation between measured and predicted values of displacement for training and testing phases are shown in Figs. 6 and 7.

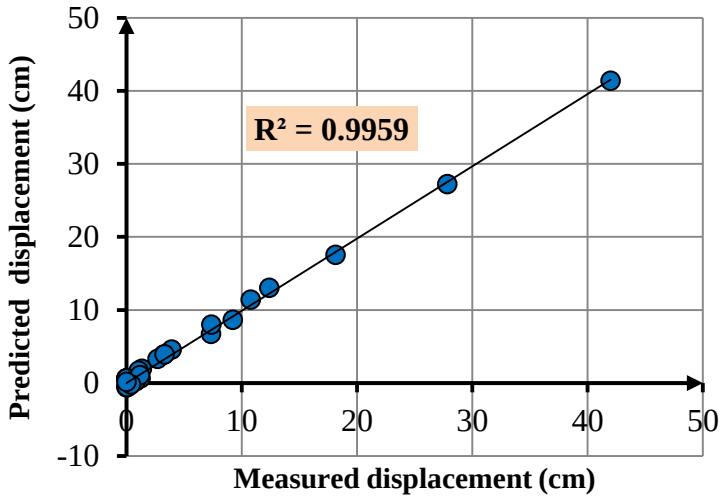

Figure 6. Correlation between measured and predicted values of displacement for training data points

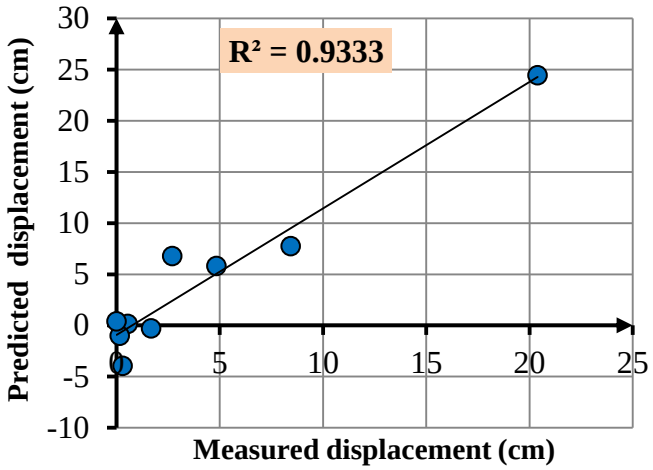

Figure 7. Correlation between measured and predicted values of displacement for testing data points

Eventually, relative error (error percentage) for data point (training and testing samples) is assessed and revealed in Fig. 8. Relative error for most data points is located in range of [-10% 10%], which is an acceptable value.

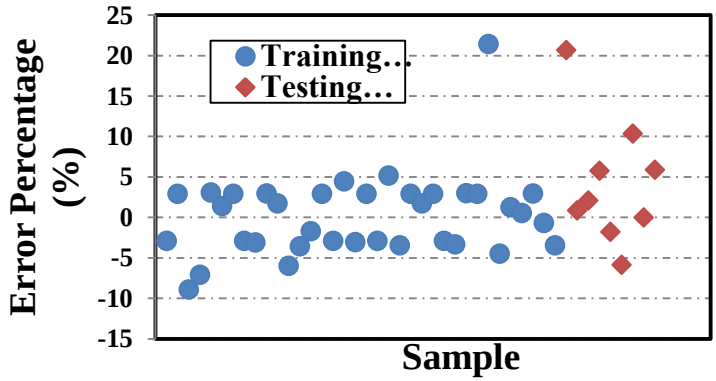

Figure 8. Relative error (error percentage) of SVR-PSO model in prediction of displacement

5. CONCLUSION

Displacements induced by earthquake are important, because displacements can be very large and result in severe damage to earth and earth supported structures. In this paper, a new approach namely support vector regression optimized by PSO is proposed for predicting the EIDS. In our methodology, PSO is applied as optimization tool for determining the optimal value of user defined parameters existing in formulation of SVR. The optimization implementation increases the performance of SVR model.

Also, examination of the error analysis shows that the presented strategy produces results with satisfactory accuracy. This study offers that SVR combined with PSO can be applied as a powerful tool for modeling of non-linear regression problems involved in civil and mining engineering.

REFERENCES

1. Ambraseys N, Srbulov M. Earthquake induced displacements of slopes. *Soil Dym Earthquake Eng* 1995; **14**: 59-71.
2. Keefer DK. Landslides caused by earthquakes. *Geolog Soci America Bull* 1984; **95**: 406-21.
3. Jibson RW. Predicting earthquake-induced landslide displacements using Newmark's sliding block analysis. *Transport Res Record* 1993;**1**: 9-17.
4. Makdisi FI, Seed HB. Simplified procedure for estimating dam and embankment earthquake-induced deformations, ASAE Publication No 4-77 Proceedings of the National Symposium on Soil Erosion and Sediment by Water, Chicago, Illinois, December, 1977.
5. Lin J-S, Whitman RV. Earthquake induced displacements of sliding blocks. *J Geotech Eng* 1986; **112**: 44-59.
6. Igarashi S, Hakuno M. The response of mass-on-rough-plane model due to earthquakes, *Proc JSCE* 1987, pp. 223-233.

7. Tika-Vassilikos TE, Sarma SK, Ambraseys NN. Seismic displacements on shear surfaces in cohesive soils, *Earthquake Eng Struct Dynam* 1993; **22**: 709-21.
8. Davis R, Desai C, Smith N. Stability of motions of translational landslides, *J Geotech Eng* 1993; **119**: 420-32.
9. Stamatopoulos C. Analysis of a slide parallel to the slope, *Proc 2nd Greek Nat Conf Geotech Eng* 1992: pp. 481-488.
10. Ambraseys N, Srbulov M. Attenuation of earthquake-induced ground displacements, *Earthquake Eng Struct Dynam* 1994; **23**: 467-87.
11. Saygili G, Rathje EM. Empirical predictive models for earthquake-induced sliding displacements of slopes. *J Geotech Geoenvironm Eng* 2008; **134**: 790-803.
12. Vapnik V. The Nature of Statistical Learning Theory: Springer, 1999.
13. Üstün B, Melssen W, Oudenhuijzen M, Buydens L. Determination of optimal support vector regression parameters by genetic algorithms and simplex optimization, *Analytica Chimica Acta* 2005; 544: 292-305.
14. 14. Meysam Mousavi S, Tavakkoli-Moghaddam R, Vahdani B, Hashemi H, Sanjari M. A new support vector model-based imperialist competitive algorithm for time estimation in new product development projects, *Robot Computer-Integrated Manufact* 2013; **29**: 157-68.
15. Holland JH. Adaptation in natural and artificial systems: an introductory analysis with applications to biology, control, and artificial intelligence: U Michigan Press, 1975.
16. Dorigo M, Birattari M. *Ant colony optimization, Encyclopedia of Machine Learning*, Springer, 2010. pp. 36-39.
17. Kaveh A, Talatahari S. Hybrid charged system search and particle swarm optimization for engineering design problems, *Eng Comput* 2011; **28**: 423-40.
18. Kaveh A, Khayatazad M. A new meta-heuristic method: ray optimization, *Comput Struct* 2012; **112**: 283-94.
19. Kaveh A, Zolghadr A. Democratic PSO for truss layout and size optimization with frequency constraints, *Comput Struct* 2014; **130**: 10-21.
20. Kaveh A, Mahdavi V. Colliding bodies optimization: a novel meta-heuristic method, *Comput Struct* 2014; **139:** 18-27.
21. Al-Anazi A, Gates I. Support vector regression for porosity prediction in a hetero-geneous reservoir: A comparative study, *Comput Geosci* 2010: **36**: 1494-503.
22. Jiang B, Zhao F. Combination of support vector regression and artificial neural networks for prediction of critical heat flux, *Int J Heat and Mass Transfer*, 2013; **62**: 481-94.
23. Wu Q, Law R. Fuzzy support vector regression machine with penalizing Gaussian noises on triangular fuzzy number space, *Expert Syst Applic* 2010; **37**: 7788-95.
24. Gunn SR. Support vector machines for classification and regression, *ISIS Technical report*, **14**(1998).
25. Vapnik V, Golowich SE, Smola A. Support vector method for function approximation, regression estimation, and signal processing. *Adv Neural Inform Process syst* 1997; **1**: 281-7.
26. Geem ZW. *Music-Inspired Harmony Search Algorithm: Theory and Applications*, Springer Verlag, 2009.
27. Eberhart R, Kennedy J. A new optimizer using particle swarm theory. , 1995 MHS'95, *Proc Sixth Int Sym Micro Mach Human Sci: IEEE* 1995. pp. 39-43.
28. Shi Y, Eberhart R. A modified particle swarm optimizer, *Evolutionary Computation Proc IEEE World Cong Comput Intell* 1998, pp. 69-73.

29. Rini DP, Shamsuddin SM, Yuhaniz SS. Particle swarm optimization: technique, system and challenges, *Int J Comput Applic* 2011; **14**: 19-26.
30. Kaveh A, Mahdavi V. Optimal design of arch dams for frequency limitations using charged system search and particle swarm optimization, *Int J Optim Civil Eng* 2011; **1**: 543-55.
31. Azad SK, Hasançebi O. Improving computational efficiency of particle swarm optimization for optimal structural design, *Int J Optim Civil Eng* 2013; **3**: 563-74.
32. Kaveh A, Nasrollahi A. Engineering design optimization using a hybrid PSO and HS algorithm, *Asian J Civil Eng* 2013; **14**: 201-23.
33. Shojaee S, Valizadeh N, Arjomand M. Isogeometric structural shape optimization using particle swarm algorithm, *Int J Optim Civil Eng* 2011; **1**: 633-45.
34. Wu C-H, Tzeng G-H, Lin R-H. A Novel hybrid genetic algorithm for kernel function and parameter optimization in support vector regression, *Expert Syst Applic* 2009; **36**: 4725-35.
35. Chen K-Y, Wang C-H. Support vector regression with genetic algorithms in forecasting tourism demand. *Tourism Manage* 2007; **28**: 215-26.
36. Huang C-L, Wang C-J. A GA-based feature selection and parameters optimizationfor support vector machines. *Expert Syst Applic* 2006; **31**: 231-40.
37. Zheng L, Zhou H, Wang C, Cen K. Combining support vector regression and ant colony optimization to reduce NOx emissions in coal-fired utility boilers. *Ener Fuels* 2008; **22**: 1034-40.
38. Hong W-C, Chen Y-F, Chen P-W, Yeh Y-H. Continuous ant colony optimization algorithms in a support vector regression based financial forecasting model, *2007 ICNC 2007 Third Int Conf Natural Comput IEEE* 2007; pp. 548-552.
39. Zheng L, Yu M. Support vector regression and ant colony optimization for combustion performance of boilers, *2008 ICNC'08 Fourth Int Conf Natural Comput IEEE* 2008, pp. 178-82.
40. Fattahi H, Gholami A, Amiribakhtiar MS, Moradi S. Estimation of asphaltene precipitation from titration data: a hybrid support vector regression with harmony search, *Neural Comput Applic* 2014; **26**: 789-98.
41. Ferentinou M, Sakellariou M. Computational intelligence tools for the prediction of slope performance, *Comput Geotech* 2007; **34**: 362-84.